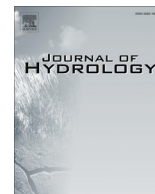


Contents lists available at [ScienceDirect](#)

Journal of Hydrology

journal homepage: [www.elsevier.com/locate/jhydrol](http://www.elsevier.com/locate/jhydrol)

## The flash flood of the Bisagno Creek on 9th October 2014: An “unfortunate” combination of spatial and temporal scales

F. Silvestro <sup>a,\*</sup>, N. Rebora <sup>a</sup>, F. Giannoni <sup>b</sup>, A. Cavallo <sup>b</sup>, L. Ferraris <sup>a,c</sup>

<sup>a</sup> CIMA Research Foundation, Savona, Italy

<sup>b</sup> ARPAL Regional Environment Protection Agency, Genova, Italy

<sup>c</sup> University of Genova, Genova, Italy

### ARTICLE INFO

#### Article history:

Available online xxxxx

#### Keywords:

Flash flood  
Probabilistic downscaling  
Catchment hydrology  
Flood forecast

### SUMMARY

On the 9th October, 2014 a strong event hit the central part of Liguria Region producing disastrous consequences to the city of Genoa where the Bisagno Creek flooded causing one death and lots of damage. The precipitation pattern responsible for the event had peculiar spatial and temporal characteristics that led to an unexpected flash flood. The temporal sequence of rainfall intensities and the particular severity of rainfall showers at small temporal scale, together with the size of the sub-basin hit by the most intense part of the rainfall were the unfortunate concurrent ingredients that led to an “almost perfect” flash flood. The peak flow was estimated to be a 100–200 years order return period.

The effects of the spatial and temporal scales of the precipitation pattern were investigated by coupling a rainfall downscaling model with a hydrological model setting up an experiment that follows a probabilistic approach.

Supposing that the correct volume of precipitation at different spatial and temporal scales is known, the experiment provided the probability of generating events with similar effects in terms of streamflow.

Furthermore, the study gives indications regarding the goodness and reliability of the forecasted rainfall field needed, not only in terms of total rainfall volume, but even in spatial and temporal pattern, to produce the observed ground effects in terms of streamflow.

© 2015 The Authors. Published by Elsevier B.V. This is an open access article under the CC BY-NC-ND license (<http://creativecommons.org/licenses/by-nc-nd/4.0/>).

### 1. Introduction

On the 9th of October 2014 another devastating flooding event affected the Bisagno Creek located in the Liguria Region in northern Italy, causing the death of one person and hundreds of millions of euro in damage to public infrastructure, buildings, private and public goods. We used the term “another” because recently another flood of similar severity struck exactly the same small catchment (Bisagno Creek), that is, 4th November 2011 (see Fig. 1); this latter event occurred only two weeks after another major event affected the eastern part of Liguria Region.

Again, the 2014 autumn season in Liguria Region, Italy was “opened” with the 9th of October, 2014 event and then marred by a series of flash flood events that affected various parts of the region. These kinds of flash floods are generated by rainfall events that are quite common in the Mediterranean area and are characterized by persistence of 4–12 h of very high intensity rainfall

structures on a small portion of the territory. The intense and localized rainfall affects small catchments ( $O(\text{Area}) \sim 10^0$  to  $10^3$  km<sup>2</sup>) that have a fast and devastating response in terms of streamflow.

Evidence of the aforementioned events can be found in the past, (Faccini et al., 2009), during the last decades they have been studied (Amengual et al., 2007; Delrieu et al., 2006; Gaume et al., 2009; Roth et al., 1996; Massacand et al., 1998; Rabuffetti et al., 2008) and especially in the last years the improvement of the measurement instruments, of the modeling systems, and of the computational capabilities allowed the scientific community to learn a lot about them, their possible causes and their effects (Argence et al., 2008; Barthlott and Kirshbaum, 2013; Brandolini et al., 2012; Buzzi et al., 2013; Davolio et al., in press; Fiori et al., 2014; Marchi et al., 2009; Rebora et al., 2013; Silvestro et al., 2012).

Lots of research have been devoted to developing, testing and applying systems to predict floods (Amengual et al., 2009; Alfieri et al., 2012; Borga et al., 2011; Jasper et al., 2002; Verbunt et al., 2007; Versini et al., 2014; Vincendon et al., 2011). The benefits of facing this issue following a probabilistic approach has been demonstrated (Bartholmes et al., 2009; Cloke and Pappenberger,

\* Corresponding author.

E-mail address: [francesco.silvestro@cimafoundation.org](mailto:francesco.silvestro@cimafoundation.org) (F. Silvestro).

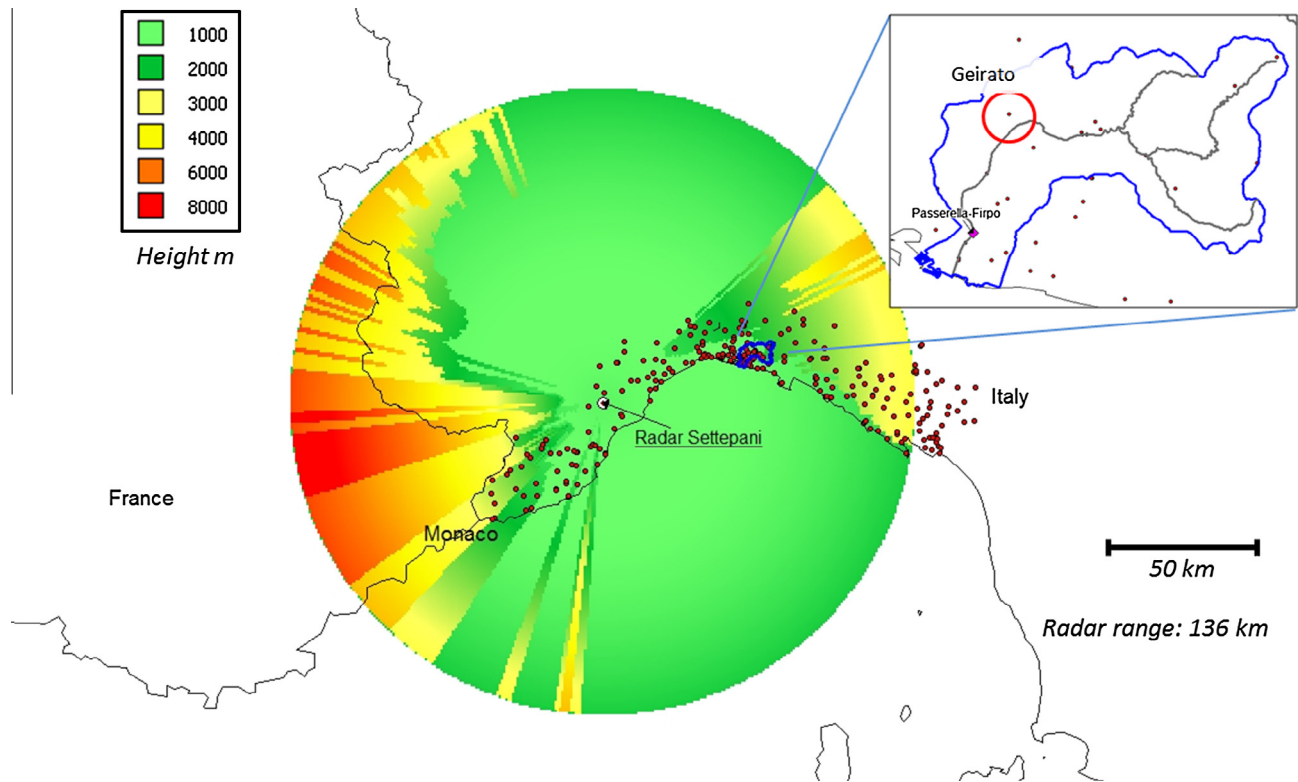


**Fig. 1.** Visibility map of the Mount Settepani radar and geo-location of study area. The watershed of the Bisagno Creek is reported (blue line) together with the main stream network (gray lines), the Passerella Firpo level gauge (violet diamond) and the rain gauge network (red dots) are also shown. The red circle evidences the Geirato rain gauge. (For interpretation of the references to color in this figure legend, the reader is referred to the web version of this article.)

2009; Ferraris et al., 2002; Krzysztofowicz, 2001; Siccardi et al., 2005). Some works investigated the advantages to follow a regional approach instead of concentrating on the forecast on a single basin (Silvestro et al., 2011; Silvestro and Rebora, 2014); this technique is called the multi-catchment probabilistic approach (Siccardi et al., 2005) and the prediction is based on the elaboration of the flood forecast made on a number of small catchments that belong to the same predefined region, in order to issue a unique forecast that is valid for the entire region.

Despite the great steps that have been taken by hydrometeorologists, it is still difficult, if not impossible, to predict with large anticipation time (12–24 h) flash floods of this sort in medium-sized and small catchments ( $O(\text{Area}) \sim 10^0$  to  $10^3$  km<sup>2</sup>). Probabilistic and regional approaches certainly help in dealing with flood forecasting, especially for operational purposes, but predicting if a particular catchment will be or will not be struck by the forecasted event is still a challenge (Buzzi et al., 2013; Silvestro et al., 2012). This is related to the difficulty and the uncertainty in predicting quantitatively reliable rainfall fields at high spatial and temporal resolutions (Buzzi et al., 2013; Brusolo et al., 2008), which is the main element that drives the flash floods that impact catchments of small dimensions.

In this paper, the flash flood event which occurred the 9th of October 2014 was analyzed in order to assess the impact of spatial and temporal patterns of rainfall in the generation of the streamflow which occurred on the Bisagno Creek. Firstly, the ability to reproduce the hydrograph using observations and modeling has been studied. Then a system made up of a probabilistic rainfall downscaling system, RainFARM (Rebora et al., 2006b) coupled with a distributed hydrological model, Continuum (Silvestro et al., 2013), was implemented and used to carry out a hydro-meteorological experiment. RainFARM was used to aggregate the

true precipitation volume observed by a meteo-radar on different reliable scales and then to disaggregate these rainfall fields to smaller scales (1 km, 10 min); Continuum was then used to transform the rainfall ensembles into streamflow scenarios.

The presented framework simulates the typical probabilistic forecast system where the rainfall predicted by a Numerical Weather Prediction System (NWPS) is given as input to a downscaling model that generates an ensemble of rainfall scenarios which are then used to drive a hydrological model (Ferraris et al., 2002; Mascaro et al., 2010; Siccardi et al., 2005). The output of NWPS is here represented by the aggregated observed rainfall fields and it is, as a consequence, supposed to be quantitatively perfectly predicted; in practice the volume of precipitation is known a priori, but only at certain spatial and temporal scales.

The results allow for the investigation of three issues: (i) the repeatability or reproducibility of the event using modeling and observations; (ii) what are the minimum temporal and spatial aggregation scales needed to generate rainfall events that result in streamflow scenarios with analogous characteristics as the one which occurred, in other words what should be the precision and detail of a NWPS in the prediction of the spatial and temporal patterns of rainfall in order to allow for the prediction of the studied event in terms of streamflow; (iii) what is the probability of generating streamflow with characteristics similar to the one which occurred, with the presented framework, depending on the aggregated spatial and temporal scales.

The article is organized as follows: in Section 2 the study area and the models used are described, Section 3 presents the experiment, while Section 4 provides a hydro-meteorological description of the event and the experiment results. In Section 5 the discussion and conclusions are presented.

## 2. Materials and methods

### 2.1. Study area and meteorological networks

Bisagno Creek is located in the center of the Liguria Region in northern Italy (Fig. 1), it drains a total area of approximately 98 km<sup>2</sup> and it is characterized by steep slopes due to the a mountainous topology given its proximity to the Apennines. The minimum and maximum elevations are 0 and 1100 m, while the mean elevation is about 370 m. The majority of the Bisagno basin is covered with vegetation characterized by forest, meadows and brushes, but the last 10 km of its river bed are heavily urbanized; there are residential areas, factories and infrastructure which are exposed to a high risk of flooding. In fact, the Bisagno Creek intersects the Genoa city centre, and the city develops along the Bisagno Creek for approximately 10 km inland. Along the last 1.5 km, towards the mouth, the river flows under a cover.

The territory of Liguria is monitored by a meteorological network, named OMIRL – “Osservatorio Meteo-Idrologico della Regione Liguria”. It is the official network managed by the Civil Protection Agency of Liguria Region and it is part of the Italian rain-gauge network managed by the Italian Civil Protection Department (Molini et al., 2009). This system provides rain-gauge measurements with 5–10 min timesteps. The network counts a total number of about 150 instruments over the region reaching an average density of 1 rain-gauge/40 km<sup>2</sup>. Stations with other sensors (temperature, radiation, wind, air humidity, etc.) are present, even though their densities are lower than the rain gauges density.

Bisagno Creek is a very well instrumented/monitored catchment with a rain gauge density of less than 1 rain-gauge/10 km<sup>2</sup>.

For the analyzed basin, level gauge data are available at the cross section Passerella Firpo that has an upstream area of about 93 km<sup>2</sup> (Fig. 1). The level data is used together with a rating curve to estimate the observed streamflow.

The Liguria Region is covered by a Doppler polarimetric C-band radar, located on Mount Settepani at an altitude of 1386 m, that works operationally with 10 min scansion time (e.g. time interval when radar data are available) (Fig. 1). Rainfall fields, provided with 1 × 1 km spatial resolution, are estimated by applying an algorithm that exploits polarimetric variables (Silvestro et al., 2009).

### 2.2. The Continuum hydrological model

Continuum (Silvestro et al., 2013, 2015) is a continuous distributed hydrological model that strongly relies on a morphological approach, based on a novel way for the drainage network components identification (Giannoni et al., 2005). The model has been conceived to be a compromise between models with a strong empirical connotation, which are easy to implement but far from reality, and complex physically based models which try to reproduce the hydrological processes with high detail but which introduce complex parameterization and consequent uncertainty and lack of robust parameters identification. It is designed to be implemented in different contexts with a special focus on data scarce environments. All of the main hydrological phenomena are modeled in a distributed way.

The basin is represented using a regular square mesh, based on Digital Elevation Model (DEM), the flow directions are identified on the basis of the directions of maximum slope derived from the DEM. The drainage network distinguishes between hillslope and channeled flow. The distinction between hillslopes and channels is made with a morphologic filter defined by the expression  $AS^k = C$  where  $A$  is the contributing area upstream of each cell [ $L^2$ ],  $S$  is the local slope [–],  $k$  and  $C$  are constants that describe

the geomorphology of the environment (Giannoni et al., 2000). This filter describes the hydrodynamic and morphological conditions in the channeled network (Giannoni et al., 2000). Infiltration and subsurface flows are described using a semi-empirical, but quite detailed, methodology based on a modification of the Horton algorithm (Bauer, 1974; Diskin and Nazimov, 1994; Gabellani et al., 2008); it accounts for soil moisture evolution even in conditions of intermittent and low-intensity rainfall (namely lower than the infiltration capacity of the soil).

The energy balance is based on the so-called “force restore equation” (Dickinson, 1988) which balances forcing and restoring terms, with explicit soil surface temperature prognostic computation.

The surface flow schematization distinguishes between channel and hillslope flows. The overland flow (hillslopes) is described by a linear reservoir scheme, while for the channel flow (channel) a schematization derived by the kinematic wave approach (Wooding, 1965; Todini and Ciarapica, 2001) is used.

Vegetation interception is schematized with a storage which has a retention capacity,  $S_v$  estimated with the Leaf Area Index data, while water table and deep flow are modeled with a distributed linear reservoir schematization and a simplified Darcy equation.

Continuum has six parameters which require calibration at the basin scale: two for the surface flow ( $u_h$  and  $u_c$ ), two for the sub-surface flow ( $c_t$  and  $c_f$ ) and two for deep flow and watertable ( $V_{Wmax}$  and  $R_f$ ) processes.

The parameter  $u_h$  influences the general shape of the hydrograph, while the impact of  $u_c$  depends on the length of the channeled paths. The parameter  $c_t$  is related to the soil field capacity and identifies the fraction of water volume in the soil that can be extracted through evapotranspiration only, while  $c_f$  controls the velocity of subsurface flow (i.e., it is related to saturated hydraulic conductivity). Both  $c_t$  and  $c_f$  regulate the dynamics of saturation of the single cells. The two parameters  $V_{Wmax}$  and  $R_f$  govern the deep flow and the watertable dynamics and have a smaller influence with respect to the other four parameters (Silvestro et al., 2013) on flood hydrographs, especially for catchments of small and medium sized drainage area.

For the current application, the model was implemented with a spatial resolution of 0.00083 deg (about 90 m) based on the Shuttle Radar Topographic Mission (SRTM) DEM. The temporal resolution used in all the experiments is 10 min.

Since the model is used in this context for flood modeling purposes, the parameters are calibrated mainly with the objective of reproducing peak flow values and time of peak. The period chosen for the calibration is 01/01/2011–31/12/2012, the performance of the calibrated parameter set (Table 1) has been evaluated referring to some standard statistics used in hydrology.

The Nash Sutcliffe (NS) coefficient (Nash and Sutcliffe, 1970):

$$NS = 1 - \frac{\sum_{t=1}^{t_{max}} (Q_m(t) - Q_o(t))^2}{\sum_{t=1}^{t_{max}} (Q_m(t) - \bar{Q}_o)^2} \quad (1)$$

where  $Q_m(t)$  and  $Q_o(t)$  are the modeled and observed streamflows at time  $t$ .  $\bar{Q}_o$  is the mean observed streamflow.

Chiew McMahon (CM) coefficient (Chiew and McMahon, 1994):

$$CM = 1 - \frac{\sum_{t=1}^{t_{max}} (\sqrt{Q_m(t)} - \sqrt{Q_o(t)})^2}{\sum_{t=1}^{t_{max}} (\sqrt{Q_m(t)} - \sqrt{\bar{Q}_o})^2} \quad (2)$$

Root Mean Square Error (RMSE):

$$RMSE = \sqrt{\frac{1}{t_{max}} \sum_{t=1}^{t_{max}} (Q_m(t) - Q_o(t))^2} \quad (3)$$

**Table 1**

Continuum parameters sets for Bisagno Creek used for simulation. Calibrated set compared with maximum and minimum values used for calibration and with the set of stressed surface parameters.

Parameter	Calibrated set	Stressed set	Min	Max
$u_c$ ( $m^{0.5}/s$ )	35	55	15	55
$u_h$ (1/s)	0.0015	0.004	0.0002	0.004
$c_t$ (-)	0.51	0.51	0.15	0.65
$c_f$ (-)	0.042	0.042	0.015	0.1
$V_{Wmax}$ (mm)	200	200	10	1500
$R_f$ (-)	1	1	0.5	30

The values of the statistics were good for the calibration period and they are reported in Table 2.

The conditions of the state variables at the beginning of the analyzed event are generated by effectuating a continuous run of the model that starts around 6 months in the past (Silvestro et al., 2013).

### 2.3. RainFARM model

RainFARM (Rebora et al., 2006a, 2006b) is a rainfall downscaling model used for generating an ensemble of precipitation fields that are consistent with large scale predictions issued by meteorological models (Laiolo et al., 2014) and/or by expert forecasters (Silvestro et al., 2011); it can reproduce the small-scale variability of precipitation needed to correctly force the rainfall–runoff model. RainFARM accounts for the spatial–temporal variability of precipitation fields at scales smaller than those at which reliable quantitative precipitation forecasts are available. RainFARM preserves the information at large scale derived from a quantitative precipitation prediction and it is able to generate small scale structures of precipitation that are consistent with radar observations of mid-latitude precipitation events.

The basic idea is that the spatial–temporal Fourier spectrum of the precipitation field, estimated at large scale from a meteorological model prediction, follows the functional form:

$$|\hat{g}(k_x, k_y, \omega)|^2 \propto (k_x^2 + k_y^2)^{-\alpha/2} \omega^{-\beta} \quad (4)$$

where  $k_x$  and  $k_y$  are the  $x$  and  $y$  spatial wavenumbers,  $\omega$  the temporal wavenumber (frequency), while  $\alpha$  and  $\beta$  represent two parameters of the model that are estimated from the power spectrum of precipitation predicted by a meteorological model on the wave numbers/frequencies that correspond to the spatial–temporal scales at which the meteorological model prediction is considered reliable.

The spectrum defined by (4) can be easily extended over larger wave numbers/frequencies thus allowing for the generation of a spatial–temporal field at a higher resolution (Rebora et al., 2006a, 2006b). The choice of random Fourier phases associated with the power spectrum (4) and the backwards transformation in real space allows for generating a stochastic ensemble of high-resolution fields that are consistent at large scale with the Quantitative Precipitation Forecast (QPF) issued by numerical models. In practice once the spatial and temporal scales where the rainfall forecast is considered reliable are defined, the downscaled rainfall

**Table 2**

Values of the statistics for the calibration period. NS: Nash Sutcliffe coefficient, CM: Chiew McMahon coefficient, RMSE: Root Mean Square Error.

Statistic	Value
NS (-)	0.79
CM (-)	0.72
RMSE ( $m^3/s$ )	0.62

field is forced to preserve both the spatial–temporal patterns and the precipitation volume at these scales; at smaller scales the rainfall field is randomly generated, but with spatial and temporal structures that are correlated in space and time with rules defined by the power spectra parameterization.

### 3. Experiment design: dealing with spatial and temporal precipitation scale in the generation of streamflow

The experiment was designed in order to analyze the influence of spatial and temporal distribution of the precipitation in the formation of the flood event which occurred, in terms of the peak flow and the time of peak flow. This should help in understanding the level of predictability of such events.

We named the system made by the rainfall downscaling model RainFARM coupled with Continuum model Flood Forecast Framework (hereafter FFF).

Fig. 2 reports the schematization of the FFF and the experiment described in the following.

We supposed that we know the volume of precipitation predicted (or observed) at a certain large scale (RV).

Since the rainfall estimated by radar provides reliable streamflow estimation (see Section 4.1), and certainly does better than the rain gauges in catching the spatial characteristics of the real rainfall field, it was used here as the “true rainfall field” (TRF).

The RainFARM parameters are estimated directly by the radar rainfall fields in order to determine the correct spatial and temporal characteristics of the rainfall event. They are constant over the event and are fitted in order to reproduce the spatial and temporal structures at the radar resolution (1 km, 10 min). In particular, the two parameters are calibrated to reproduce the spatial–temporal power spectrum of the precipitation field; this allows for the generation of an ensemble of different 3D rainfall fields with the same correlation structure as the observations.

A domain DV of  $128 \times 128$  km was considered for computational reasons.

The RVs are obtained by aggregating the TRF on the DV at different time and spatial scales (from fine to raw scales) so that the total volume of rainfall is conserved and equal to the volume of TRF when aggregated at different reliable scales (RS). This reproduces the behavior of the Numerical Weather Prediction Systems (NWPSs) that, even when they produce a good rainfall forecast, this latter is generally quantitatively reliable at certain temporal and spatial scales (Davalio et al., in press; Ferraris et al., 2002; Rebora et al., 2006b). It is, in fact, well known that due to numerical diffusion, a meteorological model is not reliable at scales smaller than six to four times its resolution (Patterson and Orszag, 1971), but this a theoretical limit and in practice, especially for variable precipitation, this reliable scale is coarser (Brussolo et al., 2008). When small-scale forcing is suitably parameterized or accounted for, for example, introducing orographic forcing, NWPSs can even render credible rainfall prediction, but in many cases the uncertainty is really elevated and often the quantitative amount and location are not sufficiently precise.

The spatial and temporal aggregation scales are chosen on one side in order to be compliant with rainfall observations (radar) and the typical NWPSs scales, on the other side to easily compute Fast Fourier Transform (FFT) transformations (Rebora et al., 2006a):

Spatial Scales (km): 1, 2, 4, 8, 16, 32, 64, 128  
Temporal Scales (min): 10, 30, 60, 180, 360, 720, 1440

The RVs are always disaggregated with RainFARM producing  $N$  equi-probable rainfall scenarios at the radar time and spatial



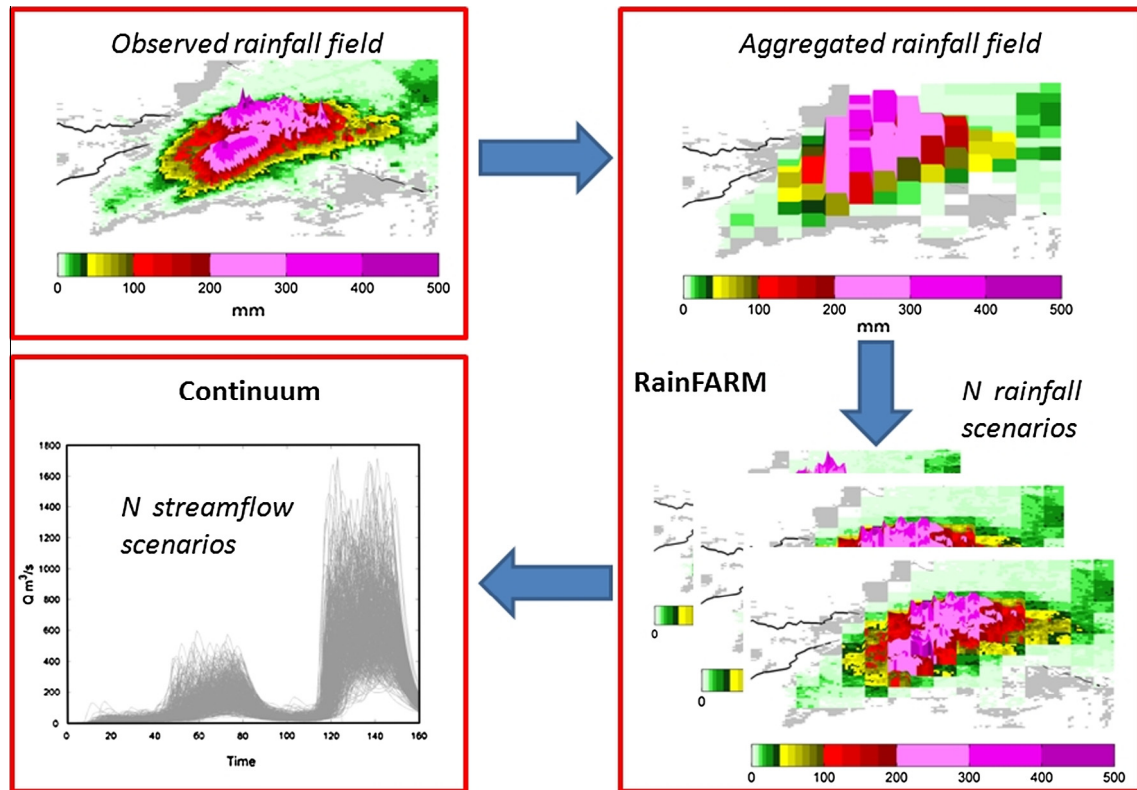


**Fig. 2.** Scheme of the Flood Forecasting Framework. Observed rainfall field is aggregated on different reliable temporal and spatial scales and then downscaled generating  $N$  rainfall scenarios. The  $N$  rainfall scenarios are used as input to the hydrological model to produce  $N$  streamflow scenarios.

resolution (1 km, 10 min) that are used to generate  $N$  equi-probable streamflow scenarios by the Continuum model. Silvestro and Reбора (2014) suggested using  $N > 50$ –100 in an operational context, to be sure to produce a statistical significant number of scenario we used  $N = 500$ .

For each couple of spatial and temporal scales (for example, spatial scale: 128 km, temporal scale 1440 min), each of the 500 high resolution rainfall field has the same spatial temporal correlation structure as the observed rainfall field. These rainfall fields have the same characteristics as the observed radar field in terms of rainfall intensities and small scale spatial patterns. When the aggregated scales are large (e.g. 128 km, 1440 min) the peaks of precipitation can occur almost everywhere in the spatial domain and in the 24 h simulation period, this case is associated with large uncertainty in a hypothetical NWPS. When the aggregation scales are small (e.g. 8 km, 180 min) the spatial and temporal localization of the event is more accurate and this case is associated with small uncertainty in an hypothetical NWPS.

The TRF is clearly aggregated even to spatial and temporal scales finer than those commonly operationally used for weather forecasting, for example the Hydro-Meteorological Functional Centre of Liguria Region (HMFC), which is in charge of hydro-meteorological forecasts for the Liguria Region, has available various NWPSs used for weather forecasting with characteristics as described in Table 3. However, this analysis aims to investigate even hypothetical scales actually not resolved, especially when considering operational systems.

In order to summarize the experiment we can state that it is mainly made by the following steps:

1. Aggregation of TRF on DV at fixed time and spatial scales obtaining RV.

**Table 3**

Characteristics of the NWPSs used by the meteorologists of HMFC to carry out the weather forecast.

Model name	Spatial resolution (km)	Temporal resolution (hours)	Lead time (days)	Type
ECMWF	30	6	6	Global Scale
COSMO-LAMI	7	3	3	Mesoscale
BOLAM	10	3	3	Mesoscale
MOLOCH	2	3	2	Regional Scale

2. Downscaling RV on radar spatial and temporal resolution with RainFARM obtaining  $N$  equi-probable rainfall scenarios.
3. Using the  $N$  equi-probable rainfall scenarios as input to Continuum to produce  $N$  equi-probable streamflow scenarios.

#### 4. The case study

##### 4.1. Hydro-meteorological description and modeling

During the 8th and the morning of 9th of October 2014 a series of regenerating storms (Bedrina et al., 2012) affected the central and eastern parts of the Liguria Region. Several showers of rainfall created peak flows in the basins in this area, but the intensities and persistence of the rainfall were not high enough to have any notable impact. On the Bisagno Creek about 130 mm of rainfall was recorded at basin scale in 36 h, produced by three main events of 3–6 h duration. During the evening of 9th of October, after some hours of very light rain, there was a new, strong and intensified storm; approximately 4 h of very intense rainfall affected the central part of the catchment causing a very fast response of the basin.

This time, 130 mm of rainfall was recorded in 4 h as average amount at basin scale, but with local rainfall amounts within the basin (on areas of only a few square kilometers) of 250 mm. Fig. 3 shows the map of the 24 h accumulated rainfall over the Bisagno Creek measured by the Settepani radar; peaks greater than 400 mm are evident, as well as the pattern of the most intense structure that struck the central and upper parts of the basin (indicated in Fig. 3 with white ellipses). The intensity of the storm is also highlighted in Fig. 4, where the 4 h accumulated rainfall from 19:00 UTC to 22:00 UTC is shown.

Fig. 5 shows the hyetograph of the rain gauge at Geirato station (see also Fig. 1 for geo-location) where an hourly rainfall peak of 130 mm was recorded.

The analysis of the instantaneous radar maps showed rainfall intensity peaks of approximately 200–250 mm/h with accumulated rainfall in 10 min of about 30–40 mm.

These very high rainfall intensities, even if for short durations, had a fundamental role in the runoff formation.

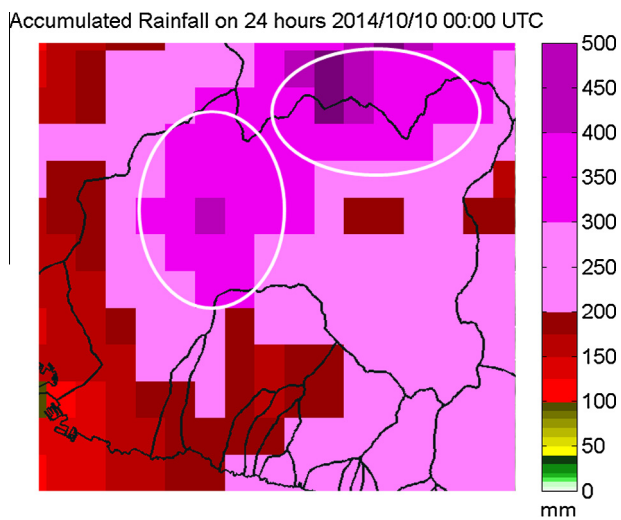


Fig. 3. Accumulated radar rainfall field over 24 h on Bisagno Creek. 9th October 00:00 UTC to 10th October 00:00 UTC. Two ellipses evidence the parts of the basin stroke by largest amounts of precipitation.

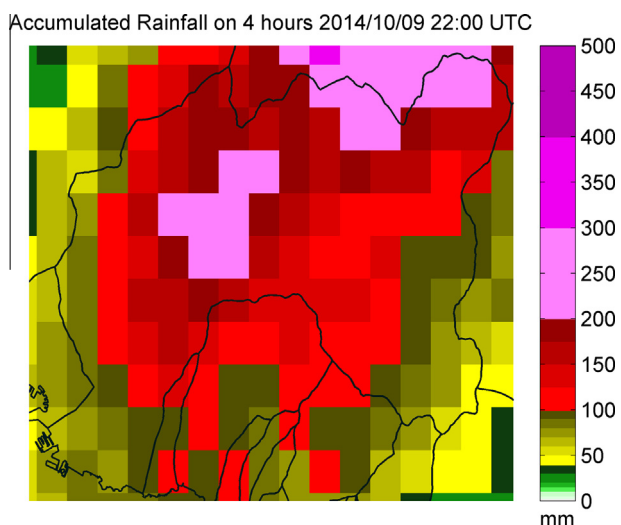


Fig. 4. Accumulated radar rainfall field over 4 h on Bisagno Creek. 9th October 19:00 UTC to 9th October 22:00 UTC.

This rainfall event led to a peak flow of about 1100–1200 m<sup>3</sup>/s that corresponds to a return period,  $T$  of approximately 100–200 yrs (Boni et al., 2007; Provincial Authority of Genoa, 2001).

The streamflow simulation to be compared with observations was carried out using four different configurations:

- (1) Simulation performed with the standard set of calibrated Continuum parameters using as input the rain gauge rainfall field with time resolution of 10 min interpolated by using Kriging method on a regular grid of 1 km resolution. The Simple (Ordinary) Kriging was used with spherical semi-variogram and the search radius around each interpolation point set to 10 km.
- (2) Simulation performed with the standard set of calibrated Continuum parameters using as input the rain gauge rainfall field with time resolution of 60 min interpolated by using the Kriging method on a regular grid of 1 km resolution
- (3) Simulation made with the standard set of calibrated Continuum parameters using as input the rainfall field estimated by the Mount Settepani radar data with time resolution of 10 min and 1 km spatial resolution
- (4) Simulation made with a stressed set of calibrated Continuum parameters using as input the rain gauge rainfall field with time resolution of 60 min interpolated with the Kriging method on a regular grid of 1 km resolution.

The configuration number 4 was obtained using very high values of surface flow parameters, which meant reducing the ground friction and increasing the water velocity on both channels and hillslopes (see Table 1). These are the parameters that have the greatest impact on the shape of the flood hydrograph. In this case, the sub-surface parameters  $c_t$  and  $c_f$  do not have a huge impact on the peak flow value, probably because when the most intense core of precipitation begins the soil was close to being saturated.

For configuration 1 the values of the performance statistics were calculated and they are reported in Table 4.

The results are presented in Fig. 6 and give us a number of interesting indications.

1. Firstly, streamflow simulations with configurations 1 and 3 (rain gauge and radar, time resolution 10 min) are good in reproducing the time and value of the peak flow as well as the general shape of the hydrograph. In both cases there is an underestimation of the low flow and an overestimation of the flood volume, the modeled hydrographs are more smoothed around the peak than the observed ones. Simulation with radar data leads to a negligible overestimation of the peak (even considering the uncertainty related to the observed flow). This result is a verification of the choice to use the radar fields in the implementation of the FFF.
2. Secondly, the rainfall fields estimated by aggregating the rainfall observations at hourly time scales produced a strong underestimation of the runoff, even though the volumes of rainfall are preserved (see configurations 1 and 2). Moreover, the peak flow splits into two close peak flows.
3. Thirdly, the runoff underestimation of configuration 2 seems poorly related to the hydrological model parameterizations. Stressing the parameters leads to an insufficient increase in the peak value and to an anticipation of the peak time, as well as to a worse shape of the hydrograph (configuration 4) emphasizing the presence of two peaks with value around 900 m<sup>3</sup>/s instead of a unique peak of about 1100 m<sup>3</sup>/s.

In summary, it seems that the spatial distribution of the precipitation (occurred with high intensities mainly in a particular sub-area of the catchment) and its temporal scale (the temporal

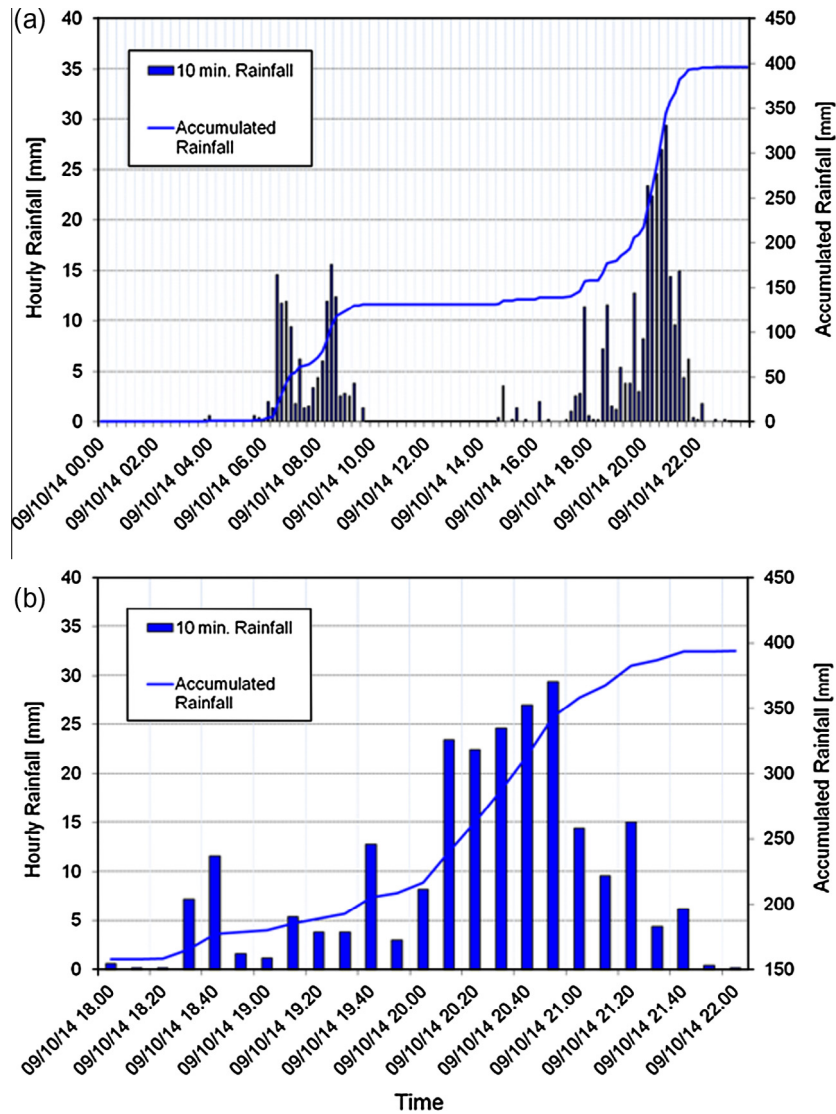


**Fig. 5.** Hyetograph measured by the Geirato rain gauge (see Fig. 1). It is the rain gauge that measured the maximum hourly accumulation during the event. One left y axis hourly accumulation is shown while right y axis reports total accumulation. Panel (a) shows the 24 h length event, panel (b) focuses on the time window with the most intense part of the event.

**Table 4**

Values of the statistics for the studied event, configuration 1. NS: Nash Sutcliffe coefficient, CM: Chiew McMahon coefficient, RMSE: Root Mean Square Error.

Statistic	Value
NS (-)	0.75
CM (-)	0.61
RMSE (m <sup>3</sup> /s)	0.56

sequence and the presence of very high intensities at very small time scale) had a significant influence on the ground effects in terms of streamflow.

#### 4.2. Experiment results

The results of the experiment described in Section 3 helped us to investigate in detail some of the issues which arose in the previous section.

The modeled streamflow obtained using radar rainfall as input to the hydrological model satisfactorily reproduced the observed hydrograph. As a result, it is used as the “reference hydrograph”

as is done quite frequently in the literature (Berenguer et al., 2005; Borga, 2002; Vieux and Bedient, 2004). In this way, we keep out of the analysis the possible uncertainties and errors introduced by hydrological modeling, even though in this case they are very small (see previous section).

We focused on the analysis of the peak values and on the time to peaks to measure how the streamflow scenarios generated by the forecast system are similar to the reference streamflow.

Fig. 7 shows the box plot of the 500 peak flows generated with FFF compared with the peak flow of the reference hydrograph ( $Q_{pr}$ ) represented by the blue<sup>1</sup> diamonds. Each panel refers to a different spatial RS (RSs), while on the x-axis the temporal RS (RSt) is reported (the case with RSs = 1 km and RSt = 10 min is obviously not considered since it corresponds to the resolution of the original field).

The graphs show that for RSs from 1 to 4 km the  $Q_{pr}$  is satisfactorily reproduced by the FFF. The box (interquartile) and whiskers have a smaller amplitude and  $Q_{pr}$  lies in their center. However this is valid only if RSt < 3 h, this means that even if the rainfall field is

<sup>1</sup> For interpretation of color in Fig. 7, the reader is referred to the web version of this article.

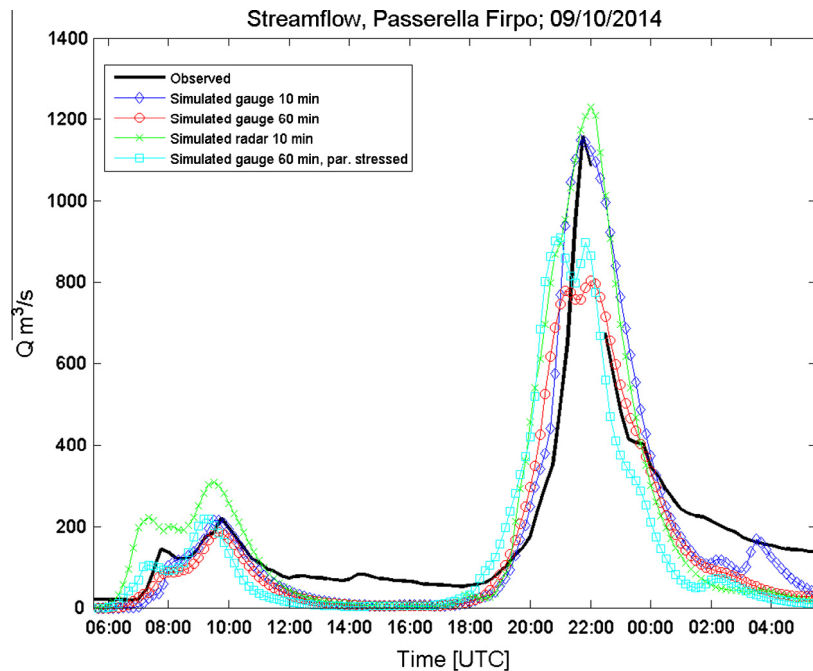


Fig. 6. Hydrograph measured and modeled in correspondence of the Passerella Firpo level gauge (area about 93 km<sup>2</sup>). The modeled hydrographs are obtained using different configurations in terms of rainfall input and model parameterization. The simulation starts the 9th October at 00:00 UTC, the figure does not show the first hours of simulations since very low streamflow values occurred.

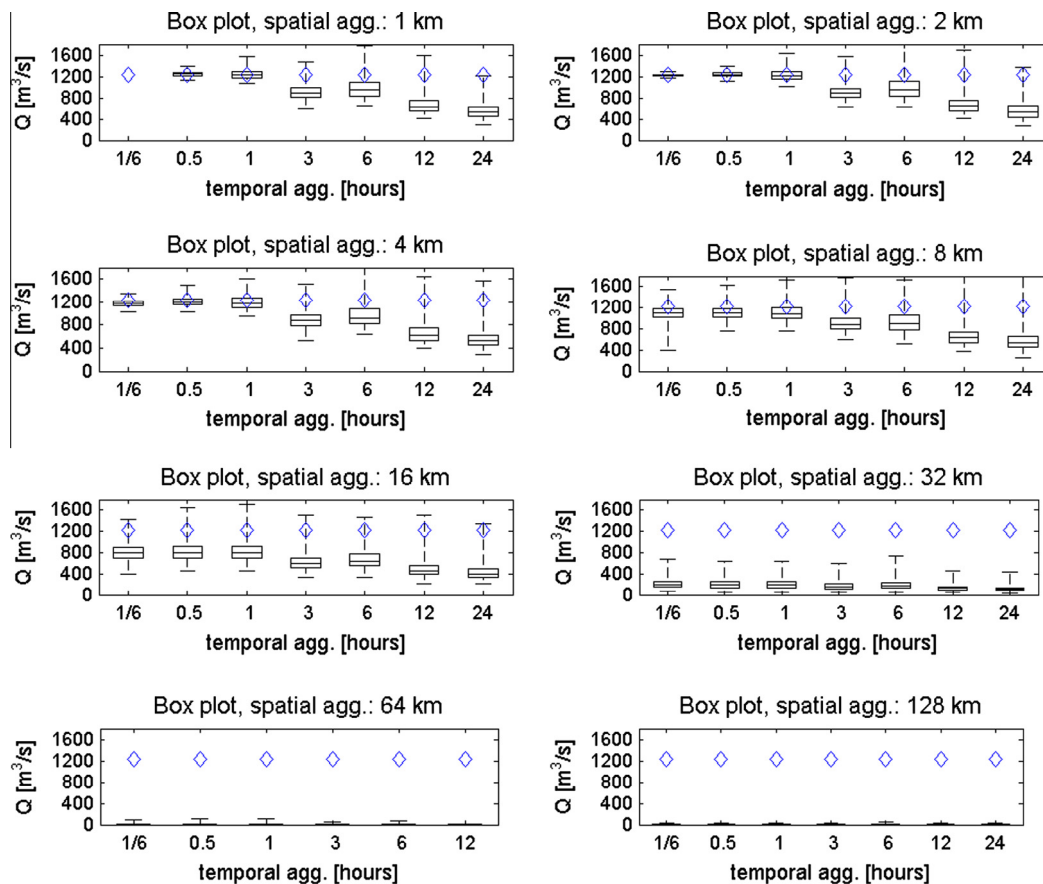


Fig. 7. Box plot of the peak flow generated by the FFF. On y axis the peak flow is reported, on x axis the temporal aggregation scales (RSt) are reported. Diamonds represent the peak flow of the reference hydrograph. Each sub-panel shows results for a different spatial aggregation scale (RSs).



known with high spatial resolution, it is fundamental to know the time sequence with great detail since it probably played a crucial role in the formation of the observed streamflow peak. For  $RSt \geq 3$  h, the  $Q_{pr}$  becomes difficult to reproduce and quite rare in the peak flow distribution (over the upper interquartile). The improvements of the results from  $RSt = 3$  h to  $RSt = 6$  h is quite interesting: this is due to the fact that the rainfall volume that caused the first peak of the hydrograph can be moved forward in time while the volume that caused the second peak of the hydrograph can be moved backward in time by RainFARM leading to a sort of compensation effect with respect to the degradation of the  $RSt$ . This does not occur for  $RSt = 3$  h because the rainfall volume is maintained constant on smaller time windows.

For  $RSs$  equal 8 and 16 km,  $Q_{pr}$  is still reproducible, but with low probability ( $Q_{pr}$  is always larger than the upper interquartile) for all  $RSt$ .

For  $RSs > 16$  km it becomes impossible to reproduce the observed event in terms of the peak flow, even when starting from a correct total volume of rainfall at the large scale.

Considering  $RSs \leq 16$  km, the FFF produces scenarios with  $Q_p > Q_{pr}$ , but these are rare. This means that the observed volume of precipitation could have caused, with low probability, a streamflow scenario which is much more dramatic than the observed flows.

All of these considerations can be confirmed by analyzing the probability plots in Fig. 8.

Each panel refers to a different  $RSs$ , on the  $x$ -axis the peak flows are reported while on the  $y$ -axis the probability is shown, different lines represent different  $RSt$ . The black vertical line is the  $Q_{pr}$ . When  $RSs$  and  $RSt$  increase the probability curves shift to the left of the graph and the probability of generating peak flows equal or larger than  $Q_{pr}$  decreases; for  $RSs$  of 1, 2, 4 km and  $Rt < 3$  h the peak flow distribution is almost centered on  $Q_{pr}$  with the probability  $P(Q_{pr})$  between 0.4 and 0.6 and a small dispersion around this value.

The fact that  $P(Q_{pr})$  dramatically decreases for  $RSs$  values between 4 and 8 km, that is, between 16 and 64 km<sup>2</sup>, confirms the need of capturing the rainfall spatial pattern on spatial scales smaller than the dimension of the basin. At the same time  $RSt < 3$  h is needed for corroborating the importance of the temporal evolution of the rainfall event. When the FFF is fed with the rainfall field aggregated at spatial scales of the order of magnitude of the basin area (8 km <  $RSs < 16$  km) the  $Q_{pr}$  becomes a rare event conditioned to the observed total volume of precipitation. From a theoretical point of view, dramatically augmenting the number of realizations (we can say  $N > 10^4$ – $10^5$ ) should lead to  $P(Q_{pr}) > 0$  even for large  $RSs$  and  $RSt$ , but  $Q_{pr}$  would remain an extremely rare streamflow value.

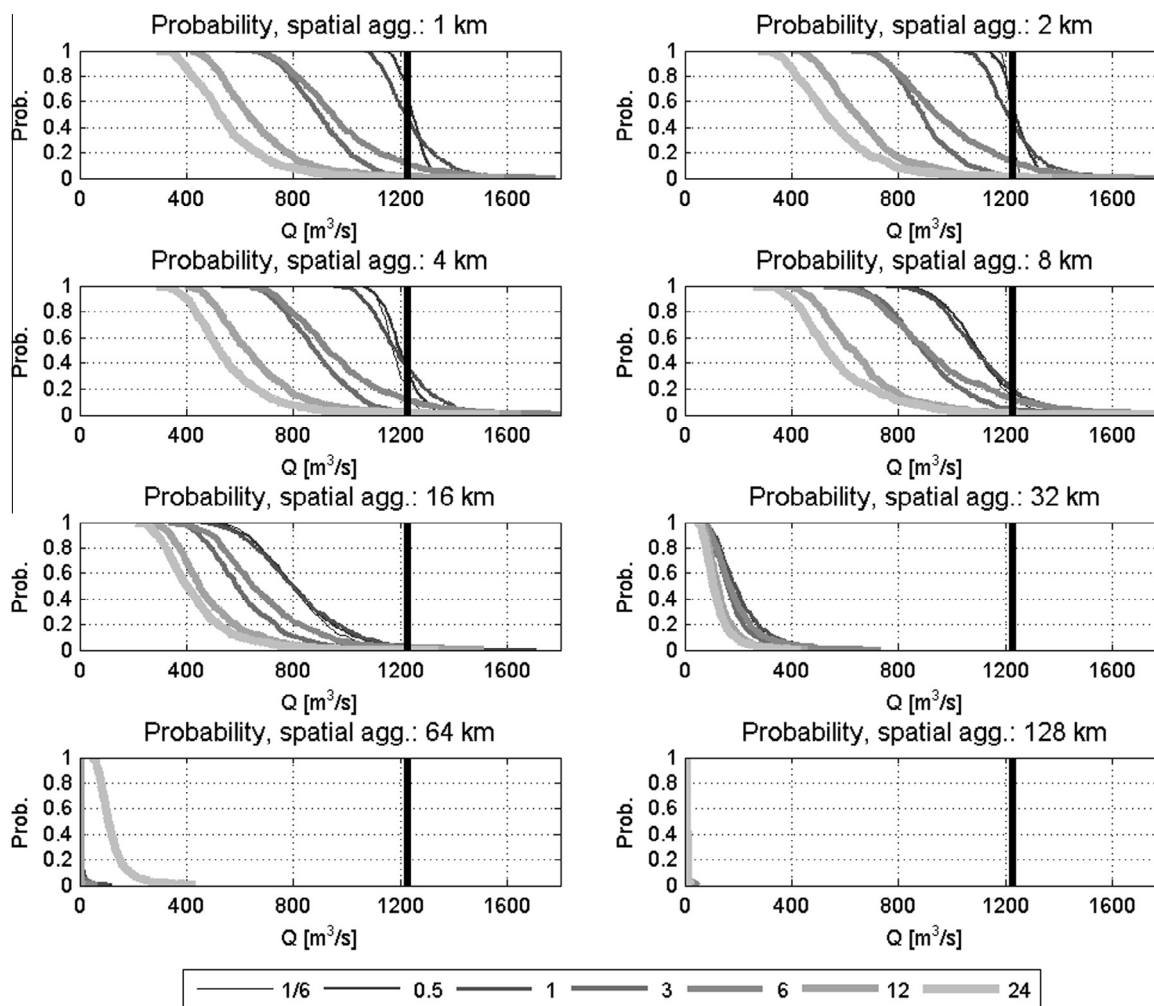


**Fig. 8.** Probability curves of the peak flow generated by the FFF. On  $x$  axis the peak flow is reported, on  $y$  axis the probability is reported. Each sub-panel shows results for a different spatial aggregation scale ( $RSs$ ). Different curves for a fixed sub-panel represent different temporal aggregation scales ( $RSt$ ).

Figures similar to Figs. 7 and 8 have been built referring to the time to peak. In this case, the considered aleatory variable is:

$$dT_p = T_{pm} - T_{pr} \quad (5)$$

where  $T_{pr}$  is the time to peak of the reference hydrograph and  $T_{pm}$  is the modeled time to peak.  $dT_p$  is 0 when the peak time is perfectly reproduced by the modeled streamflow.

Fig. 9 reports the box plot of the variable  $dT_p$  as a function of RSs and RSt. The upper and lower interquartile of  $dT_p$  is lower than 1 h for RSs from 1 to 16 km and RSt < 3 h, this is an interesting fact because it means that the time to peak is satisfactorily reproduced even for RSs 8 and 16 km, but for these latter the magnitude of the peak ( $Q_{pr}$ ) is difficult to model (see Figs. 7 and 8). When RSt is low the temporal evolution of rainfall and streamflow is satisfactorily reproduced, so it is possible to satisfactorily model the  $T_p$ , but to reproduce even the  $Q_{pr}$  with high probability we need to know the rainfall pattern at fine spatial scale (RSs < 8).

When RSt increases,  $dT_p$  tends to be negative because the observed peak is at the end of the event while the downscaling model changes the temporal location of the most intense cores of the rainfall inside the RSt time window.

Fig. 10 represents the probability distribution curves of  $dT_p$ , the step shape of the graphs is due to the time step of the hydrological model which is discrete (10 min).

For small RSs and RSt, the curves rapidly decrease and the probability of large  $dT_p$  (positive or negative) is very low or null, while for large RSs the curves are always flat. When RSt increases the probability curves become flat and extend the range on the

negative values of the x-axis more than the positive values, this is again due to the temporal evolution of the studied event.

#### 4.3. Issues about the impact of aggregation scales on final results

For the sake of clarity we want to highlight the fact that there may be some effects on the final results presented in Section 4.2 due to the process of rainfall aggregation and disaggregation, especially when the aggregation scales RSs and RSt are large.

The first issue is related to aggregation spatial scale; since the domain is centered on radar location, even when the aggregation scale is 128 km the box does not include area for which there are not observed data, anyway the effect of bounding box could theoretically impact on final results. In fact, supposing to have an observed rainfall field that cover a domain much larger than the one of Settepani radar, we could shift on x and y axis the grid where we aggregate the rainfall field modifying the volume of precipitation to be disaggregated. Anyway this is the condition that occurs when one wants to downscale the rainfall field derived from a operational NWPS, that generally has the spatial calculation grid fixed.

The second issue is related to the temporal scale; when RSt is larger than certain values, that generally depend by the rainfall temporal evolution and by the dimension of the studied basin, the results are sensitive to the start time of the aggregation period.

Finally the downscaling methodology assumes that the rainfall probability distribution function is the same everywhere in the domain that is a simplification of the real physical process.

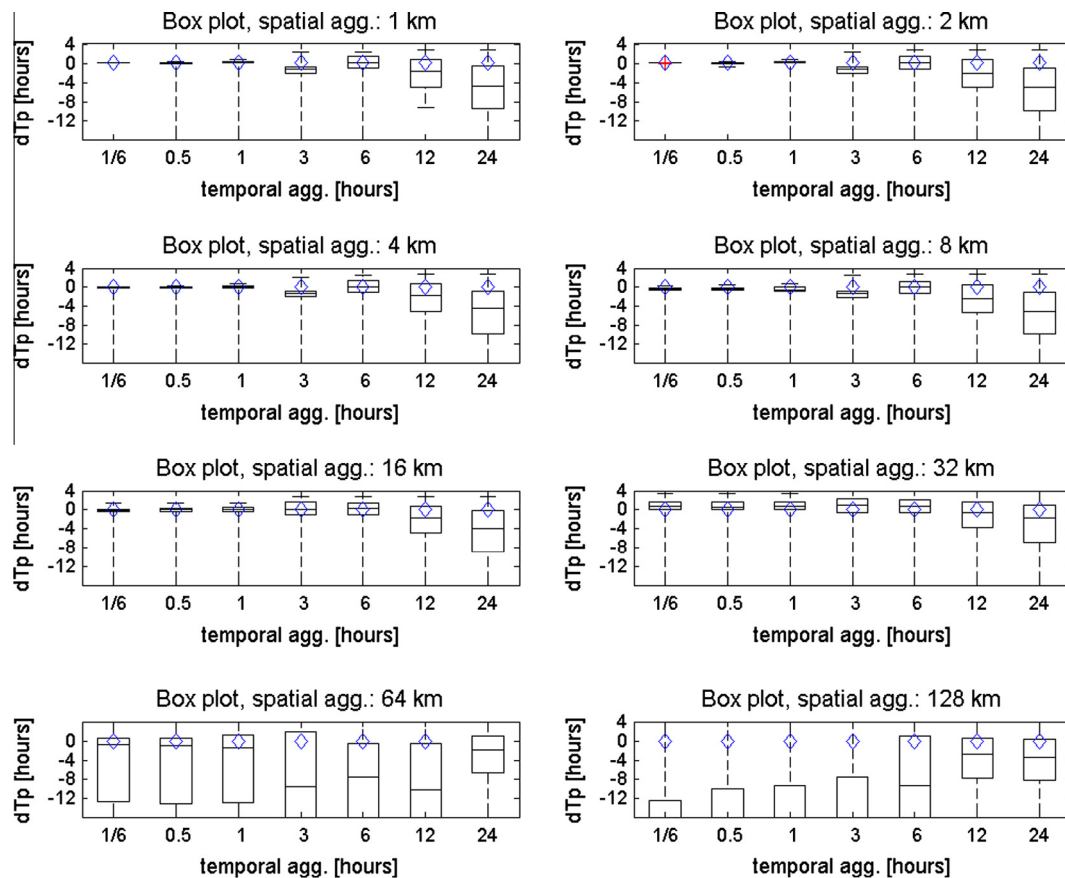
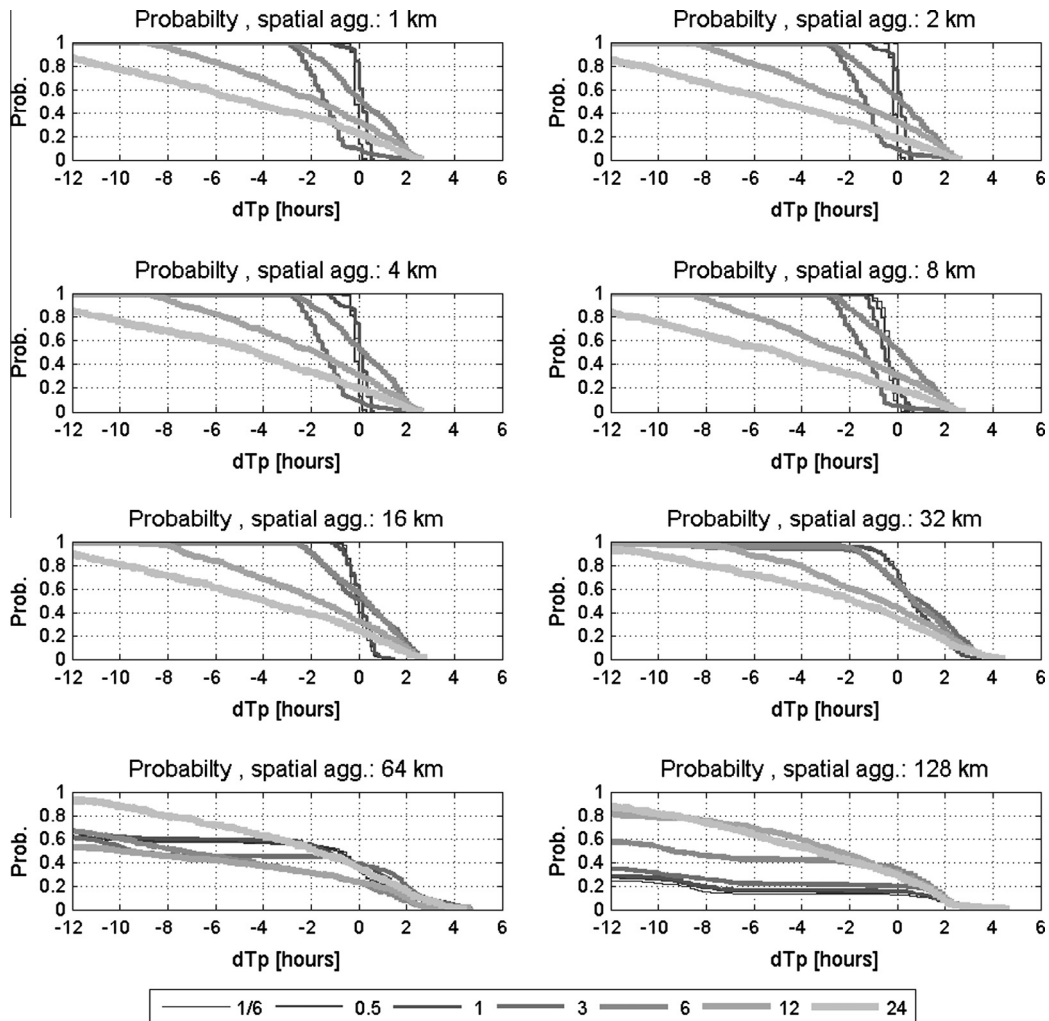


Fig. 9. Box plot of the variable  $dT_p$ : difference between the time to peak of the reference hydrograph and the time to peak of the streamflow series generated by the FFF. On y axis the  $dT_p$  is reported, on x axis the temporal aggregation scales (RSt) are reported. Diamonds represent the  $dT_p$  of the reference hydrograph, which is 0. Each sub-panel shows results for a different spatial aggregation scale (RSs). For a better readability of the graphs we fixed  $-6$  to  $6$  h as y axis limits.



**Fig. 10.** Probability curves of the variable  $dT_p$ : difference between the time to peak of the reference hydrograph and the time to peak of the streamflow series generated by the FFF. On  $x$  axis the  $dT_p$  is reported, on  $y$  axis the probability is reported. Each sub-panel shows results for a different spatial aggregation scale (RSs). Different curves for a fixed sub-panel represent different temporal aggregation scales (RSt).

For the analyzed test case we believe that the results for  $RSs > 32$  km and  $RSt > 1-3$  h are presumably sensitive to the above mentioned factors, anyway the final findings of the analysis would not sensitively change.

## 5. Discussion and conclusions

In this work, we analyzed the major flood event which affected the Bisagno Creek in Liguria Region, Italy on the 9th October, 2014. We tried to investigate how the temporal and spatial pattern of rainfall impacted on the runoff generation and streamflow evolution.

This has been done by: (i) modeling the event using rain gauge and radar rainfall estimations as input to a hydrological model; (ii) setting up an experiment using a probabilistic flood forecast framework based on a rainfall downscaling model and a hydrological model. The true rainfall volume derived by radar rainfall estimation has been aggregated to different spatial and temporal scales (RSs and RSt) and then disaggregated to the original scale in order to evaluate the reproducibility and predictability of the event in a probabilistic forecast context.

The analysis of the results leads to some interesting considerations.

The rainfall temporal patterns on fine time steps (10 min) played a fundamental role in the runoff formation and the magnitude of the observed streamflow peak. Using rainfall aggregated to hourly time steps to feed the Continuum hydrological model leads to an underestimation of the peak flow.

The reliable spatial scale RSs needed to reproduce the observed peak flow with reasonable probability (we can say  $P(Q_p > Q_{pr}) = 0.2$  or larger) must be smaller than 8 km, beyond that (RSs 8–16 km),  $Q_{pr}$  becomes quite a rare event that is generated only by a reduced number of ensemble members,  $P(Q_p > Q_{pr}) = 0.05-0.2$ ; when  $RSs > 16$  km it becomes almost impossible to generate  $Q_{pr}$ .

The temporal evolution of precipitation had a crucial role in the peak flow formation, in fact for RSt larger or equal to 3 h the probability of generating  $Q_{pr}$  rapidly decreases for all RSs.

The optimal configurations are  $RSs \leq 2$  km and  $RSt \leq 1$  h, in these cases the probability distribution of  $Q_p$  is almost centered on the  $Q_{pr}$ .

All these considerations demonstrated that to predict the correct magnitude of the peak flow observed during the analyzed event it is not sufficient to predict the correct volume of precipitation, it is essential to predict also the spatial and temporal pattern at a fine scale. This occurs even in the case of working in a probabilistic framework where the possibility of downscaling the rainfall field from a coarse to a fine scale exists.

It is probably an overstatement to say that it was a “perfect storm”, but the results seem to suggest that the observed volume of rainfall occurred according to an improbable (in a certain sense unfortunate) combination of temporal and spatial scales.

The findings of the experiment give some indications about the predictability of the event and show that forecasting the effects of the event in terms of streamflow was very difficult because it was necessary to have very detailed rainfall predictions, which are probably still difficult to obtain steadily with large anticipation (12–24 h) by existing NWPSs (Buzzi et al., 2013). Moreover, the results confirm that for predicting flash floods on small basins the multi-catchment approach, based on forecasting at the regional scale (grouping the catchments) and not on the single catchment (Siccardi et al., 2005), is fundamental. In this kind of environment, made by a collection of very small catchments, decision makers are obliged to face the impossibility of identifying a specific catchment as the target of the warning to be issued; the only effective option is issuing warnings at the regional or sub-regional scale (Silvestro and Rebola, 2014).

### Acknowledgements

This work is supported by the Italian Civil Protection Department and by the Italian Region of Liguria. We are very grateful to all the meteorologists and the hydrologists of the Meteo-Hydrologic Centre of Liguria Region, for the many useful discussions we had. We are grateful to Garvin Cummings for his suggestions in reviewing the quality of the writing.

### References

- Alfieri, L., Thielen, J., Pappenberger, F., 2012. Ensemble hydro-meteorological simulation for flash flood early detection in southern Switzerland. *J. Hydrol.* 424–425, 143–153. <http://dx.doi.org/10.1016/j.jhydrol.2011.12.038>.
- Amengual, A., Romero, R., Gomez, M., Martin, A., Alonso, S., 2007. A hydrometeorological modeling study of a flash-flood event over Catalonia, Spain. *J. Hydrometeorol.* 8, 282–303.
- Amengual, A., Romero, R., Vich, M., Alonso, S., 2009. Inclusion of potential vorticity uncertainties into a hydrometeorological forecasting chain: application to a medium size basin of Mediterranean Spain. *Hydrol. Earth Syst. Sci.* 13 (6), 793–811.
- Argence, S., Lambert, D., Richard, E., Chaboureaud, J.P., Sohne, N., 2008. Impact of initial condition uncertainties on the predictability of heavy rainfall in the Mediterranean: a case study. *Q. J. R. Meteorol. Soc.* 134, 1775–1788.
- Barthlott, C., Kirshbaum, D.J., 2013. Sensitivity of deep convection to terrain forcing over Mediterranean islands. *Q. J. R. Meteorol. Soc.* 139, 1762–1779.
- Bartholmes, J.C., Thielen, J., Ramos, M.H., Gentilini, S., 2009. The European flood alert system EFAS – Part 2: statistical skill assessment of probabilistic and deterministic operational forecasts. *Hydrol. Earth Syst. Sci.* 13, 141–153. <http://dx.doi.org/10.5194/hess-13-141-2009>.
- Bauer, S., 1974. A modified Horton equation during intermittent rainfall. *Hydrol. Sci. Bull.* 19, 219–229.
- Bedrina, T., Parodi, A., Quarati, A., Clematis, A., 2012. ICT approaches to integrating institutional and non-institutional data services for better understanding of hydro-meteorological. *Nat. Hazards Earth Syst. Sci.* 12, 1961–1968.
- Berenguer, M., Corral, C., Sanchez-Diesma, R., Sempere-Torres, D., 2005. Hydrological validation of a radar-based nowcasting technique. *J. Hydrometeorol.* 6, 532–549.
- Boni, G., Ferraris, L., Giannoni, F., Roth, G., Rudari, R., 2007. Flood probability analysis for un-gauged watersheds by means of a simple distributed hydrologic model. *Adv. Water Resour.* 30 (10), 2135–2144. <http://dx.doi.org/10.1016/j.advwatres.2006.08.009>.
- Borga, M., 2002. Accuracy of radar rainfall estimates for streamflow simulation. *J. Hydrol.* 267, 26–39.
- Borga, M., Anagnostou, E.N., Blöschl, G., Creutin, J.D., 2011. Flash flood forecasting, warning and risk management: the HYDRATE project. *Environ. Sci. Policy* 834–844.
- Brandolini, P., Cevasco, A., Firpo, M., Robbiano, A., Sacchini, A., 2012. Geo-hydrological risk management for civil protection purposes in the urban area of Genoa (Liguria, NW Italy). *Nat. Hazards Earth Syst. Sci.* 12, 943–959.
- Brussolo, E., von Hardenberg, J., Ferraris, L., Rebola, N., Provenzale, A., 2008. Verification of quantitative precipitation forecasts via stochastic downscaling. *J. Hydrometeorol.* 9, 1084–1094.
- Buzzi, A., Davolio, S., Malguzzi, P., Drofa, O., Mastrangelo, D., 2013. Heavy rainfall episodes over Liguria of autumn 2011: numerical forecasting experiments. *Nat. Hazards Earth Syst. Sci. Discuss.* 1, 7093–7135.
- Chiew, F., McMahon, T., 1994. Application of the daily rainfall–runoff model MODHYDROLOG to 28 Australian catchments. *J. Hydrol.* 153, 383–416.
- Cloke, H.L., Pappenberger, F., 2009. Ensemble flood forecasting: a review. *J. Hydrol.* 375 (3–4), 613–626.
- Davolio, S., Silvestro, F., Malguzzi, P., 2015. Effects of increasing horizontal resolution in a convection permitting model on flood forecasting: the 2011 dramatic events in Liguria (Italy). *J. Hydrometeorol.* (in press). <http://dx.doi.org/10.1175/JHM-D-14-0094.1>.
- Delrieu, G., Ducrocq, V., Gaume, E., Nicol, J., Payrastré, O., Yates, E., Kirstetter, P.E., Andrieu, H., Ayrat, P.-A., Bouvier, C., Creutin, J.-D., Livet, M., Anquetin, S., Lang, M., Neppel, L., Obled, C., Parent-du-Châtelet, J., Saulnier, G.M., Walpersdorf, A., Wobrock, W., 2006. The catastrophic flash-flood event of 8–9 September 2002 in the Gard Region, France: a first case study for the Cévennes-Vivarais Mediterranean Hydrometeorological Observatory. *J. Hydrometeorol.* 6, 34–52.
- Dickinson, R., 1988. The force–restore method for surface temperature and its generalization. *J. Clim.* 1, 1086–1097.
- Diskin, M.H., Nazimov, N., 1994. Linear reservoir with feedback regulated inlet as a model for the infiltration process. *J. Hydrol.* 172, 313–330.
- Faccini, F., Piccazzo, M., Robbiano, A., 2009. Natural hazards in San Fruttuoso di Camogli (Portofino Park, Italy): a case study of a debris flow in a coastal environment. *Italian J. Geosci.* 128, 641–654.
- Ferraris, L., Rudari, R., Siccardi, F., 2002. The uncertainty in the prediction of flash floods in the northern Mediterranean environment. *J. Hydrometeorol.* 3, 714–727.
- Fiori, E., Comellas, A., Molini, L., Rebola, N., Siccardi, F., Gochis, D.J., Tanelli, S., Parodi, A., 2014. Analysis and hindcast simulations of an extreme rainfall event in the Mediterranean area: the Genoa 2011 case. *Atmos. Res.* 138, 13–29.
- Gabellani, S., Silvestro, F., Rudari, R., Boni, G., 2008. General calibration methodology for a combined Horton–SCS infiltration scheme in flash flood modeling. *Nat. Hazards Earth Syst. Sci.* 8, 1317–1327.
- Gaume, E., Bain, V., Bernardara, P., Newinger, O., Barbuc, M., Bateman, A., Blaskovicova, L., Blöschl, G., Borga, M., Dumitrescu, A., Daliakopoulos, I., Garcia, J., Irimescu, A., Kohnova, S., Koutroulis, A., Marchi, L., Matreata, S., Medina, V., Preciso, E., Sempere-Torres, D., Stancalie, G., Szolgay, J., Tsanis, I., Velasco, D., Viglione, A., 2009. A compilation of data on European flash floods. *J. Hydrol.* 367, 70–78.
- Giannoni, F., Roth, G., Rudari, R., 2000. A semi-distributed rainfall–runoff model based on a geomorphologic approach. *Phys. Chem. Earth* 25 (7–8), 665–671.
- Giannoni, F., Roth, G., Rudari, R., 2005. A procedure for drainage network identification from geomorphology and its application to the prediction of the hydrologic response. *Adv. Water Resour.* 28 (6), 567–581. <http://dx.doi.org/10.1016/j.advwatres.2004.11.013>.
- Jasper, K., Gurtz, J., Lang, H., 2002. Advanced flood forecasting in Alpine watersheds by coupling meteorological observations and forecasts with a distributed hydrological model. *J. Hydrol.* 267, 40–52.
- Krzysztofowicz, R., 2001. The case for probabilistic forecasting in hydrology. *J. Hydrol.* 249, 2–9.
- Laiolo, P., Gabellani, S., Rebola, N., Rudari, R., Ferraris, L., Ratto, S., Stevenin, H., Cauduro, M., 2014. Validation of the Flood-PROOFS probabilistic forecasting system. *Hydrol. Process.* 28, 3466–3481. <http://dx.doi.org/10.1002/hyp.9888>.
- Marchi, L., Borga, M., Preciso, E., Sangati, M., Gaume, E., Bain, V., Delrieu, G., Bonnifait, L., Pogancik, N., 2009. Comprehensive post-event survey of a flash flood in Western Slovenia: observation strategy and lessons learned. *Hydrol. Process.* 23 (26), 3761–3770. <http://dx.doi.org/10.1002/hyp.7542>.
- Mascaro, G., Vivoni, E.R., Deidda, R., 2010. Implications of ensemble quantitative precipitation forecast errors on distributed streamflow forecasting. *J. Hydrometeorol.* 11, 69–86.
- Massacand, A.C., Wernli, H., Davies, H.C., 1998. Heavy precipitation on the alpine southside: an upper-level precursor. *Geophys. Res. Lett.* 25, 1435–1438.
- Molini, L., Parodi, A., Siccardi, F., 2009. Dealing with uncertainty: an analysis of the severe weather events over Italy in 2006. *Nat. Hazards Earth Syst. Sci.* 9, 1–13.
- Patterson, G., Orszag, S., 1971. Spectral calculations of isotropic turbulence: efficient removal of aliasing interaction. *Phys. Fluids* 14, 2538–2541.
- Provincial Authority of Genoa, 2001. River Basin Planning of the Bisagno Creek. <<http://cartogis.provincia.genova.it/cartogis/pdb/bisagno>>.
- Rabuffetti, D., Ravazzani, G., Corbari, C., Mancini, M., 2008. Verification of operational Quantitative Discharge Forecast (QDF) for a regional warning system – the AMPHORE case studies in the upper Po River. *Nat. Hazards Earth Syst. Sci.* 8, 161–173.
- Rebola, N., Ferraris, L., Hardenberg, J.H., Provenzale, A., 2006a. Rainfall downscaling and flood forecasting: a case study in the Mediterranean area. *Nat. Hazards Earth Syst. Sci.* 6, 611–619.
- Rebola, N., Ferraris, L., Hardenberg, J.H., Provenzale, A., 2006b. The RainFARM: rainfall downscaling by a filtered auto regressive model. *J. Hydrometeorol.* 7 (4), 724–738.
- Rebola, N., Molini, L., Casella, E., Comellas, A., Fiori, E., Pignone, F., Siccardi, F., Silvestro, F., Tanelli, S., Parodi, A., 2013. Extreme rainfall in the Mediterranean: what can we learn from observations? *J. Hydrometeorol.* 14, 906–922.
- Roth, G. et al., 1996. The STORM project: aims, objectives and organisation. *Remote Sens. Rev.* 14, 23–50.
- Siccardi, F., Boni, G., Ferraris, L., Rudari, R., 2005. A hydro-meteorological approach for probabilistic flood forecast. *J. Geophys. Res.* 110, d05101. <http://dx.doi.org/10.1029/2004jd005314>.
- Silvestro, F., Rebola, N., 2014. Impact of precipitation forecast uncertainties and initial soil moisture conditions on a probabilistic flood forecasting chain. *J. Hydrol.* 519, 1052–1067.



- Silvestro, F., Reborá, N., Ferraris, L., 2009. An algorithm for real-time rainfall rate estimation by using polarimetric radar: RIME. *J. Hydrometeorol.* 10, 227–240.
- Silvestro, F., Reborá, N., Ferraris, L., 2011. Quantitative flood forecasting on small and medium size basins: a probabilistic approach for operational purposes. *J. Hydrometeorol.* 12 (6), 1432–1446.
- Silvestro, F., Gabellani, S., Giannoni, F., Parodi, A., Reborá, N., Rudari, R., Siccardi, F., 2012. A hydrological analysis of the 4th November 2011 event in Genoa. *Nat. Hazards Earth Syst. Sci.* 12, 2743–2752. <http://dx.doi.org/10.5194/nhess-12-2743-2012>.
- Silvestro, F., Gabellani, S., Delogu, F., Rudari, R., Boni, G., 2013. Exploiting remote sensing land surface temperature in distributed hydrological modelling: the example of the Continuum model. *Hydrol. Earth Syst. Sci.* 17, 39–62. <http://dx.doi.org/10.5194/hess-17-39-2013>.
- Silvestro, F., Gabellani, S., Delogu, F., Rudari, R., Laiolo, P., Boni, G., 2015. Uncertainty reduction and parameter estimation of a distributed hydrological model with ground and remote-sensing data. *Hydrol. Earth Syst. Sci.* 19, 1727–1751. <http://dx.doi.org/10.5194/hess-19-1727-2015>.
- Todini, E., Ciarapica, L., 2001. The TOPKAPI model. In: Singh, V.P. et al. (Eds.), *Mathematical Models of Large Watershed Hydrology*. Water Resources Publications, Littleton, Colorado (Chapter 12).
- Verbunt, M., Walser, A., Gurtz, J., Montani, A., Schär, C., 2007. Probabilistic flood forecasting with a limited-area ensemble prediction system: selected case studies. *J. Hydrometeorol.* 8, 897–909. <http://dx.doi.org/10.1175/JHM594.1>.
- Versini, P.A., Berenguer, M., Corral, C., Sempere-Torres, D., 2014. An operational flood warning system for poorly gauged basins: demonstration in the Guadalhorce basin (Spain). *Nat. Hazards* 71, 1355–1378.
- Vieux, B.E., Bedient, P.B., 2004. Assessing urban hydrologic prediction accuracy through event reconstruction. *J. Hydrol.* 299, 217–236.
- Vincendon, B., Ducrocq, V., Nuissier, O., Vié, B., 2011. Perturbation of convection-permitting NWP forecasts for flash-flood ensemble forecasting. *Nat. Hazards Earth Syst.* 11, 1529–1544.
- Wooding, R.A., 1965. A hydraulic modeling of the catchment-stream problem. 1. Kinematic wave theory. *J. Hydrol.* 3, 254–267.